

# Simulations of Binary Black Hole Mergers

**Dale Choi**

NASA Goddard Space Flight Center

Greenbelt, MD

In collaboration with

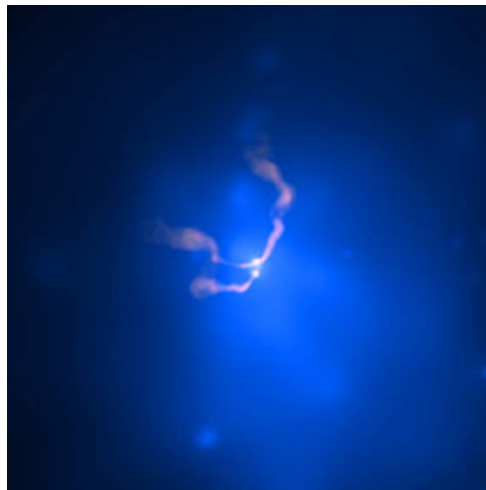
J. Centrella, J. Baker, M. Koppitz, J. van Meter (NASA/GSFC) & M. C. Miller (UMD)

# Outline

- Introduction
- Methods: Hahndol code
- Results and analysis

# Introduction

- Einstein's theory of general relativity predicts existence of black holes and gravitational waves.
- Black holes provide central engines of most active galactic nuclei and play significant roles in formation and evolution of galaxies and various dynamical phenomena such as jets.
- As a result of galactic mergers, binary black hole system will be formed that can eventually merge into a single black hole emitting gravitational waves.



Composite X-ray(blue) and Radio (pink) image of Abell 400 galaxi cluster

# Introduction

- Gravitational waves can “penetrate” deep into the center of the sources and convey direct information about dynamics of the sources.
- GW is the most direct way to map out spacetime geometry around black holes.
- Binary black hole systems are among the main sources of gravitational wave observatories such as LIGO/VIRGO/GEO and LISA.
- Main motivation for simulations of Binary black hole (BBH) systems is to provide theoretical models/templates for the GW signal.
  - LIGO: S/N for detection of signals can be greatly improved with accurate template in the merger regime.
  - LISA: Errors in extraction of source parameters and tests of strong-field GR can be reduced with the more accurate modeling of waveforms.
- Understanding of early inspiral phase and late ringdown phase are mostly under control. However, understanding of “merger” phase of BBH coalescence, which requires numerical relativity simulations, has been very difficult and became possible only very recently.

# Methods: HAHNDOL code

- A version of BSSN system of equations with evolution variables  $\{\tilde{\gamma}_{ij}, \phi, \tilde{A}_{ij}, K, \tilde{\Gamma}^i\}$  defined from the usual ADM variables  $\{\gamma_{ij}, K_{ij}\}$ .

$$\begin{aligned}\phi &= \frac{1}{12} \log \gamma \\ K &= \gamma^{ab} K_{ab} \\ \tilde{\gamma}_{ij} &= e^{-4\phi} \gamma_{ij} \\ \tilde{A}_{ij} &= e^{-4\phi} \left( K_{ij} - \frac{1}{3} \gamma_{ij} K \right) \\ \tilde{\Gamma}^i &= \tilde{\gamma}^{ab} \tilde{\Gamma}_{ab}^i\end{aligned}$$

where  $\tilde{\Gamma}_{ab}^i$  Christoffel symbol associated with the conformal metric  $\tilde{\gamma}_{ij}$ .

# Hahndol Code

## Equation of motion

$$\begin{aligned}
 \frac{d\phi}{dt} &= -\frac{1}{6}\alpha K \\
 \frac{dK}{dt} &= -\nabla^a \nabla_a \alpha + \alpha \left( \tilde{A}_{ab} \tilde{A}^{ab} + \frac{1}{3} K^2 \right) \\
 \frac{d\tilde{\gamma}_{ij}}{dt} &= -2\alpha \tilde{A}_{ij} \\
 \frac{d\tilde{A}_{ij}}{dt} &= e^{-4\phi} (-\nabla_i \nabla_j \alpha + \alpha R_{ij})^{\text{TF}} + \alpha \left( K \tilde{A}_{ij} - 2\tilde{A}_{ia} \tilde{A}^a_j \right) \\
 \frac{\partial \tilde{\Gamma}^i}{\partial t} &= 2\alpha \left( \tilde{\Gamma}_{ab}^i \tilde{A}^{ab} - \frac{2}{3} \tilde{\gamma}^{ia} K_{,a} + 6\tilde{A}^{ia} \phi_{,a} \right) \\
 &\quad - \tilde{\Gamma}^j \beta^i_{,j} + \frac{2}{3} \tilde{\Gamma}^i \beta^j_{,j} + \beta^k \tilde{\Gamma}^i_{,k} \\
 &\quad + \tilde{\gamma}^{jk} \beta^i_{,jk} + \frac{1}{3} \tilde{\gamma}^{ij} \beta^k_{,kj} - 2\tilde{A}^{ia} \alpha_{,a} - \left( \chi_{yo} + \frac{2}{3} \right) \left( \tilde{\Gamma}^i - \tilde{\gamma}^{kl} \tilde{\Gamma}^i_{kl} \right) \beta^m_{,m}
 \end{aligned}$$

where  $d/dt = \partial/\partial t - \mathcal{L}_\beta$ . The last term in  $\tilde{\Gamma}^i$  equation suggested by Yo et al to suppress exponential growth of  $\tilde{\Gamma}^i$  when  $\beta^j_{,j} > 0$ . But we find most recently that this term may not be necessary.

# Hahndol code

- Black holes represented by “punctures” at  $t = 0$ .
  - $\phi = \phi_{BL} + \phi_{reg}, \phi_{BL} = 1 + \sum_{n=1}^2 \frac{m_n}{2|\vec{r} - \vec{r}_n|}$  where the  $n^{th}$  black hole has mass (parameter)  $m_n$  and is located at coordinate  $\vec{r}_n$ .
- For  $t > 0$ , we do NOT make this “separation” (i.e. no special treatment for the closed form part,  $\phi_{BL}$ ) but directly finite-difference the whole  $\phi$ .
- May generate non-convergence/lower-order convergence near “punctures”. But, in practice, puncture “errors” remain inside the horizon and do not influence the dynamics outside the horizon.
- Combined with proper choices of gauges, this strategy is proven to be a robust way to realize moving black hole idea.
- Currently do not use black hole excision technique.

# Hahndol code

- Gauge conditions do NOT change dynamics, but may affect degree of difficulties with which the solutions from numerical evolutions can be obtained.
- Gauge conditions: specify  $\alpha, \beta^i$ .

$$\begin{aligned}\partial_t \alpha &= -2\alpha K + \beta^i \partial_i \alpha \\ \partial_t \beta^i &= \frac{3}{4} \alpha B^i \\ \partial_t B^i &= \partial_t \tilde{\Gamma}^i - \beta^j \partial_j \tilde{\Gamma}^i - \eta B^i\end{aligned}$$

- Improved version being used now (van Meter, Baker, Koppitz, Choi 2006, PRD, accepted)

$$\begin{aligned}\partial_t \alpha &= -2\alpha K + \beta^i \partial_i \alpha \\ \partial_t \beta^i &= \frac{3}{4} B^i + \beta^j \partial_j \beta^i \\ \partial_t B^i &= \partial_t \tilde{\Gamma}^i - \beta^j \partial_j (\tilde{\Gamma}^j - B^j) - \eta B^i\end{aligned}$$

# Initial Data: Quasi-circular orbit

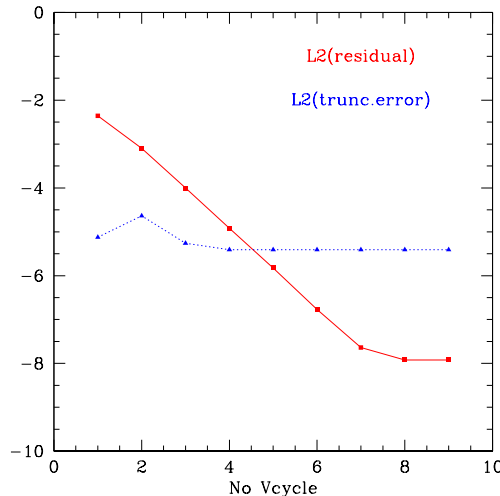
- Assume conformal flatness and maximal slicing ( $\tilde{\gamma}_{ij} = \eta_{ij}, K = 0$ )
- Bowen York form of extrinsic curvature

$$K^{ij} = \frac{3}{2r^2} (P^i n^j + P^j n^i - (\gamma^{ij} - n^i n^j) P^k n_k) + \frac{3}{r^3} (\epsilon^{ikl} S_k n_l n^j + \epsilon^{jkl} S_k n_l n^i)$$

- Puncture method: split  $\phi = \phi_{BL} + u$  and solve for  $u$ .

$$\Delta u + \beta \left(1 + \frac{u}{\phi_{BL}}\right)^{-7} = 0, \beta = \frac{1}{8} \phi_{BL}^{-7} K^{ij} K_{ij}$$

- Use multigrid algorithm.



# Waveform Analysis

- Use NP Weyl tensor component  $\Psi_4$  to analyse (outgoing) gravitational wave content.
- Harmonic decomposition

$$\Psi_4(r, \theta, \phi, t) = \sum_{lm} A_{lm}(r, t) {}_{-2}Y_{lm}(\theta, \phi)$$

$$A_{lm}(r, t) = \int \Psi_4(r, \theta, \phi, t) {}_{-2}Y_{lm}(\theta, \phi) d\Omega$$

- Given  $\Psi_4$ , one can calculate  $E, J_z, P_z$ .

$$E = \frac{r^2}{4\pi} \int \int_{\Omega} \left| \int_{-\infty}^t dt' \Psi_4(t', r, \theta, \phi) \right|^2 d\Omega dt$$

$$P_z = \frac{r^2}{4\pi} \int \int_{\Omega} \cos \theta \left| \int_{-\infty}^t dt' \Psi_4(t', r, \theta, \phi) \right|^2 d\Omega dt$$

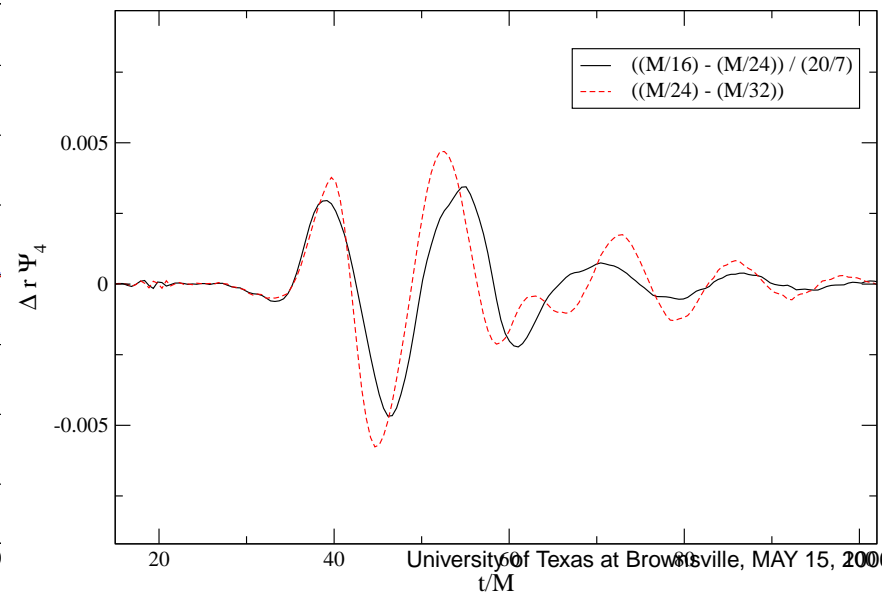
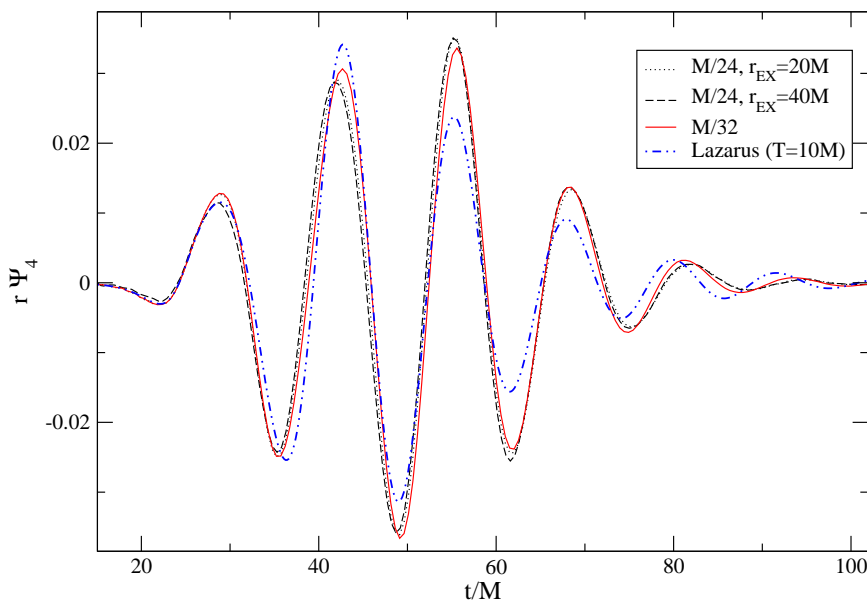
$$J_z = -\frac{r^2}{4\pi} \int \operatorname{Re} \left[ \int_{\Omega} d\Omega (\partial_{\phi} \int_{-\infty}^t dt' \psi_4(t', r, \theta, \phi)) \right. \\ \left. \times \left( \int dt' \int d\tilde{t} \bar{\psi}_4(\tilde{t}, r, \theta, \phi) \right) \right] dt$$

# Some numerical details

- Initial Data: MultiGrid algorithm.
- Evolution: Finite difference method
  - Spatial differencing: 4th order (centered/upwind)
  - Time integration: iterative Crank Nicholson / RK4 time integrator.
- Outer Boundary: causally disconnected from the region of spacetime we are interested. Simple out-going wave boundary conditions are used.
- Use PARAMESH package to implement parallelism and adaptivity.
- Performance: scaling is good  $\sim 90 - 95\%$  level up to 1000 CPUs.
- Runs take 1–5 days on 256/512 CPUs.

# Results: Inspiral $L/M \sim 4.99$ “QC0”

- Baker, Centrella, Choi, Koppitz, van Meter, Phys. Rev. Lett. **96**, 111102 (2006)
- Initial data based on Cook (1994):  $L/M = 4.99$ ,  $J/M^2 = 0.779$  with  $M$  total (initial) ADM mass.
- Grid set-up: FMR with MR boundaries located at  $2M, 4M, 8M, 16M, 32M, 64M$  with OB at  $128M$
- Resolutions run:  $h_f = M/16, M/24, M/32$
- Confirmed solution convergence and waveform convergence



# Results: Inspirals with larger $L/M$

- Baker, Centrella, Choi, Koppitz, van Meter, Phys. Rev. **D73**, 104002 (2006)
- Consider initial data with a larger separation than “QC0”.
- $L/M = 9.9, 11.1, 12.1, 13.2$  (Runs: R1, R2, R3, R4)
- Grid set-up
  - Initially grids are set-up by hand (FMR)
  - During the evolution, adaptive mesh refinement based on a function called the real part of Coulomb scalar  $\chi$ . In terms of the curvature invariants  $I$ ,  $J$ , and  $S$ ,

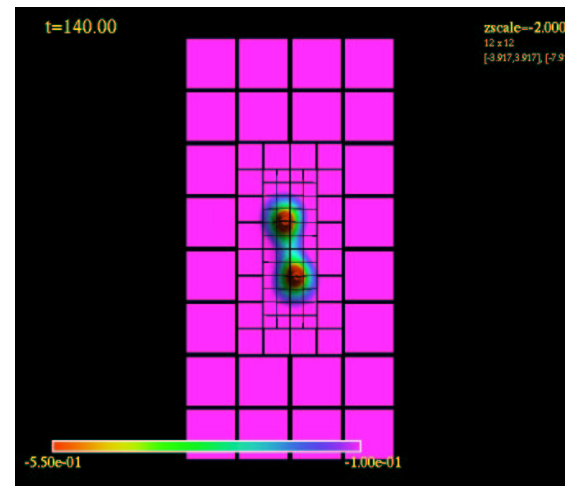
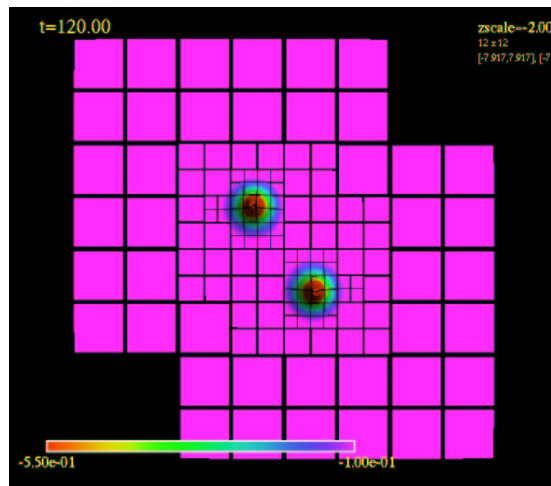
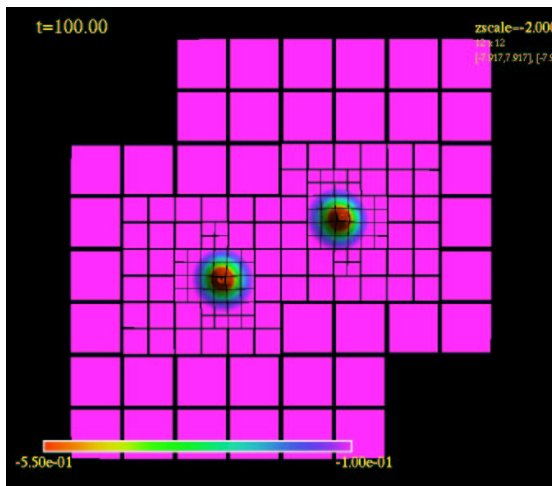
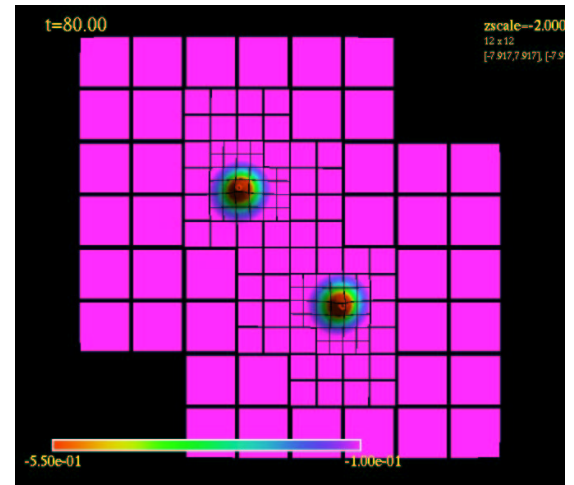
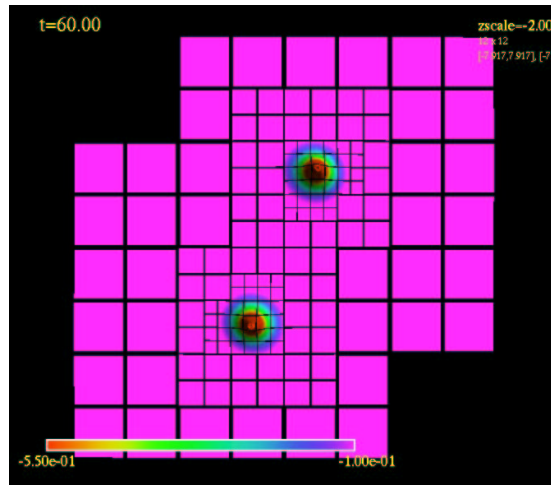
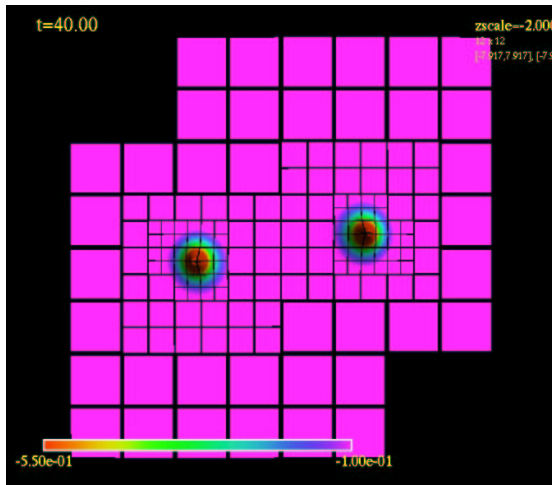
$$\chi = -\frac{3J \left( W^{\frac{1}{3}} + W^{-\frac{1}{3}} \right)}{2I\sqrt{S}}$$
$$W \equiv \sqrt{S} - \sqrt{S-1}$$

# Results: R1–R4

- Question I: can we separate initial data transient part of the waveforms from the actual merger waveforms?
- Answer I: agreement between waveforms from different runs indicate that initial data transients go away during the first orbit or so and QC0 initial separation is too small.
- Question II: what is the dependence of waveforms on the initial data with increasing separation? are there any features in the actual merger waveforms?
- Answer II: Remarkable agreement for the last orbit, merger and ringdown for all runs. There seems to be universal features. All the memory about the initial data seems to be washed away.

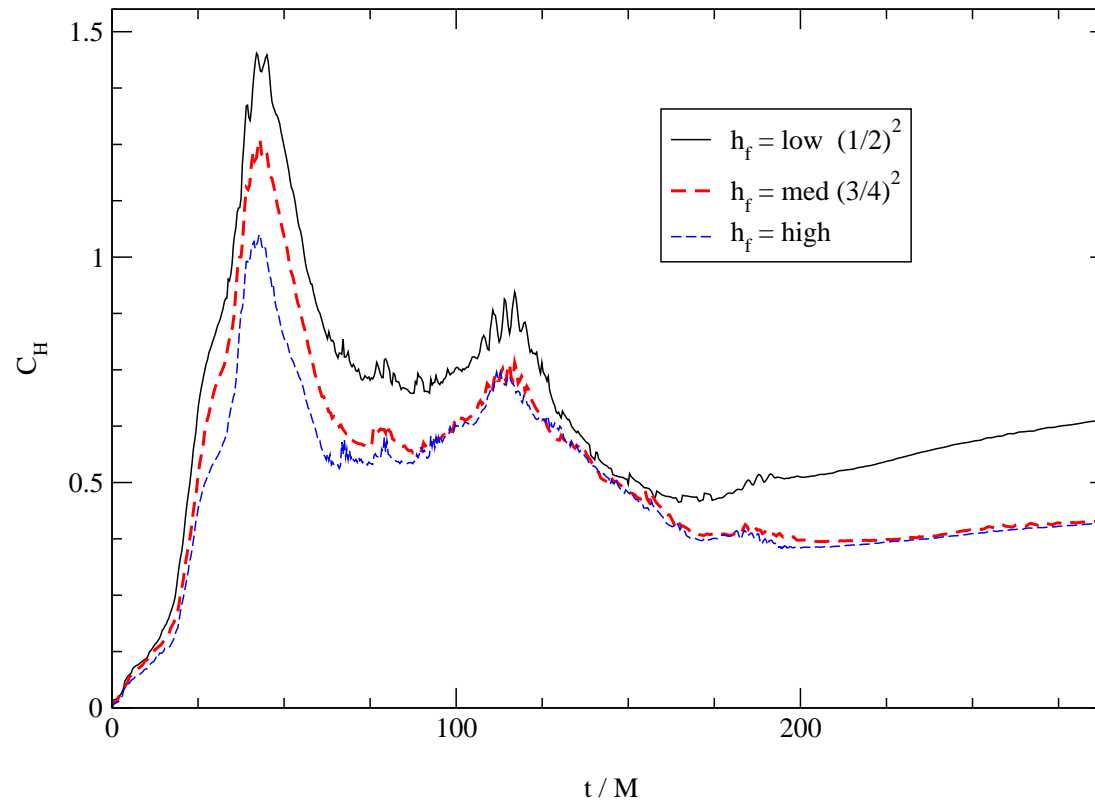
# Results: Solution R1

- Snapshots of grid structure:  $\text{Re}(\chi)$  on  $z = 0$  plane at  $t = 40M, 60M, 80M, 100M, 120M, 140M$  [MOVIE 1]



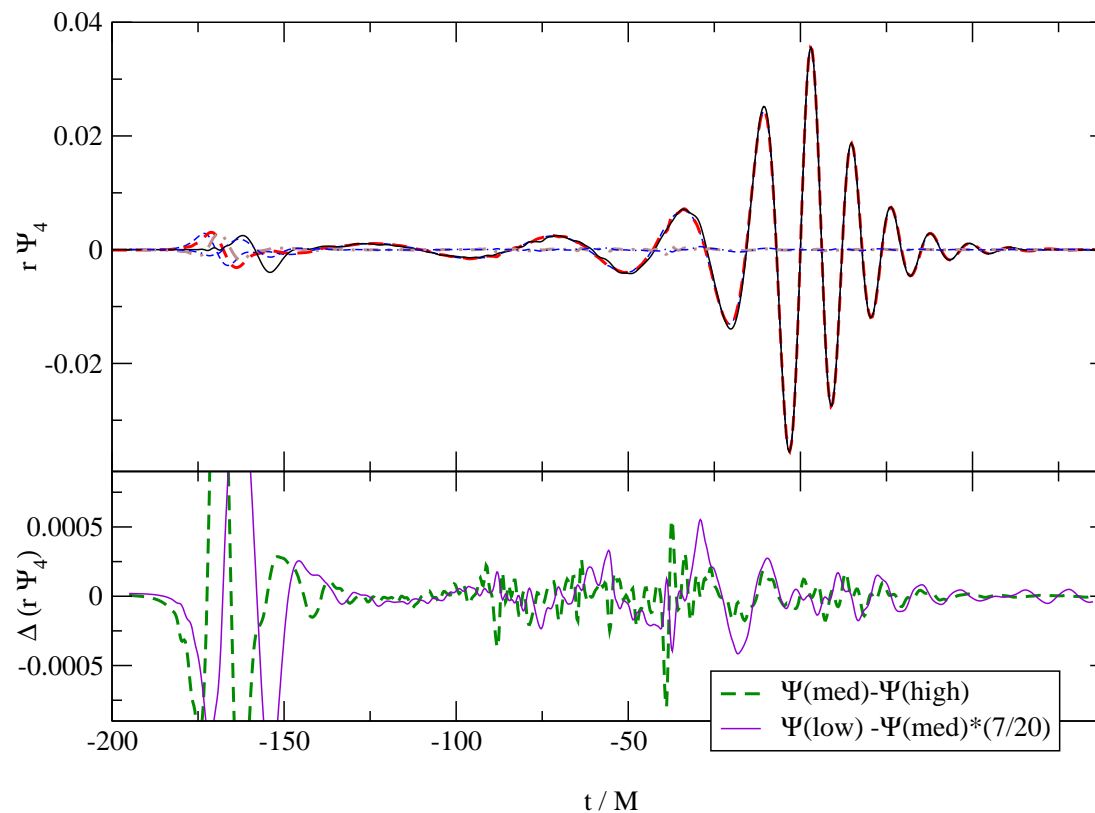
# Results: R1 HC errors

- R1 runs: Hamiltonian Constraint errors. Resolutions:  $h_f = 3M/64, M/32, 3M/128$ .



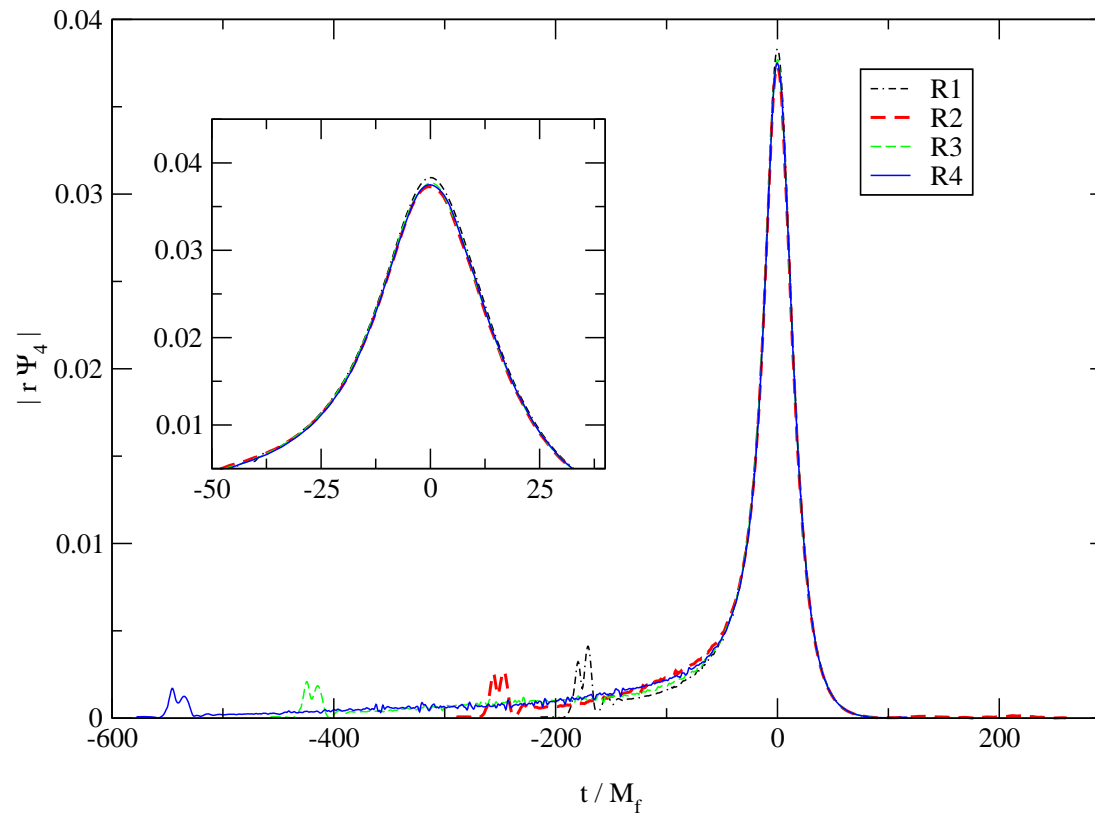
# Results: Gravitational Waveforms

- R4 run: [MOVIE 2]
- R1 runs: Errors in Gravitational Waveforms



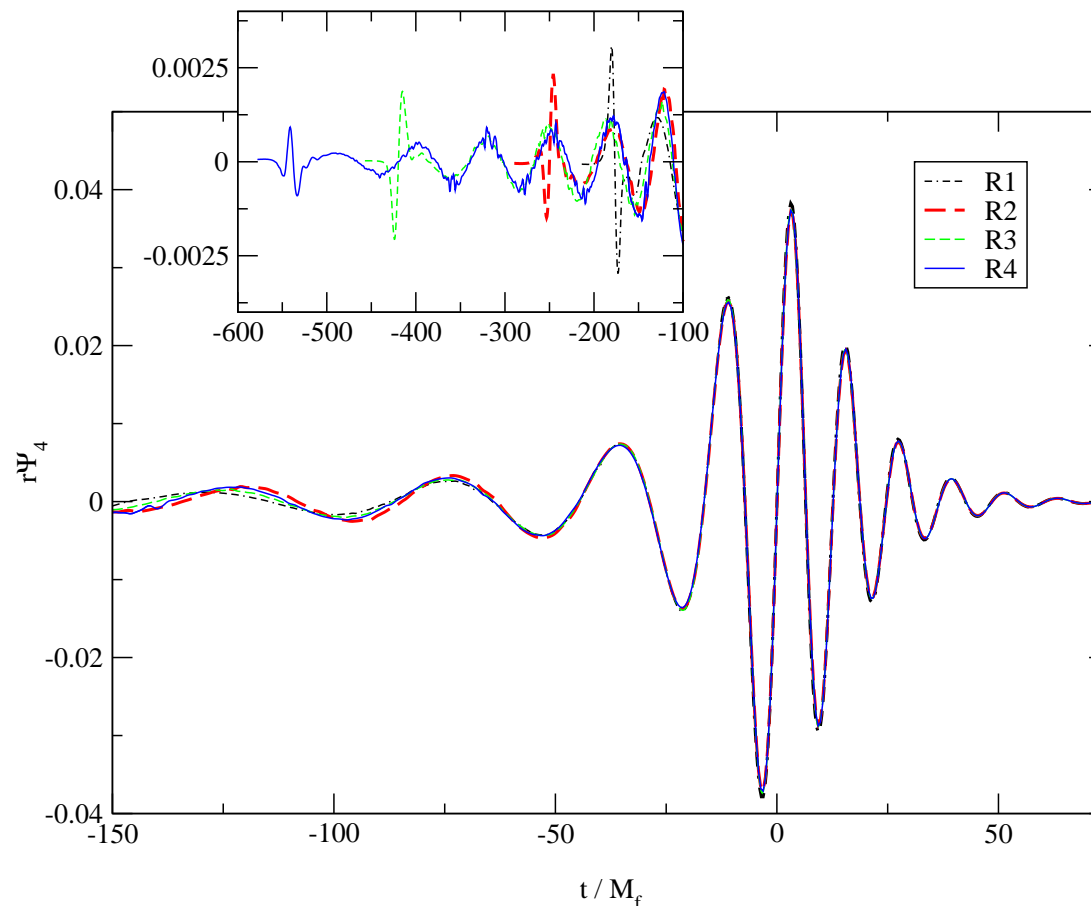
# Results: Wave amplitude from R1–R4

- $r\Psi_4(t) = A(t)\exp(-i\varphi(t))$
- Waveform amplitude,  $A(t)$ . (Time-shifted to match the maximum amplitude.)



# Results: Waveforms from R1–R4

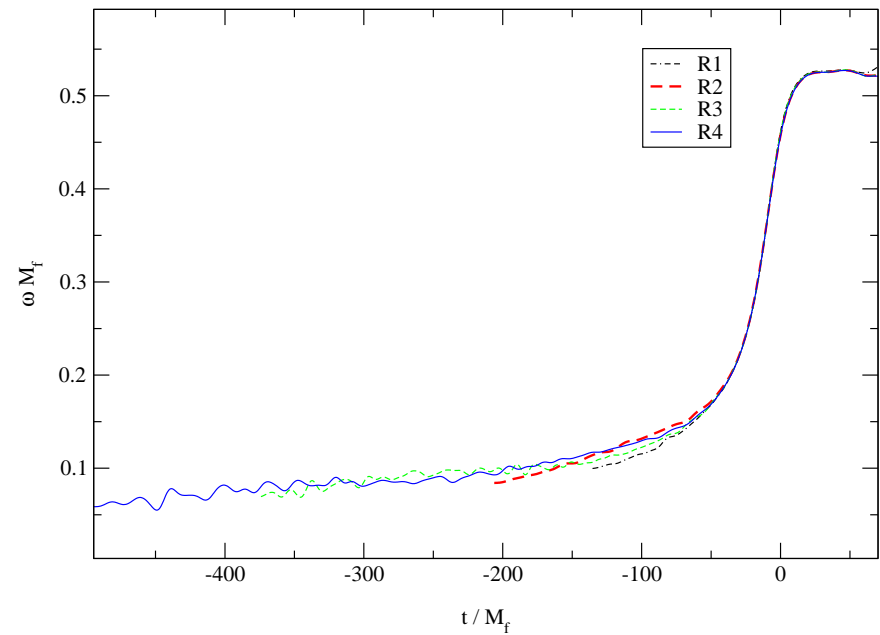
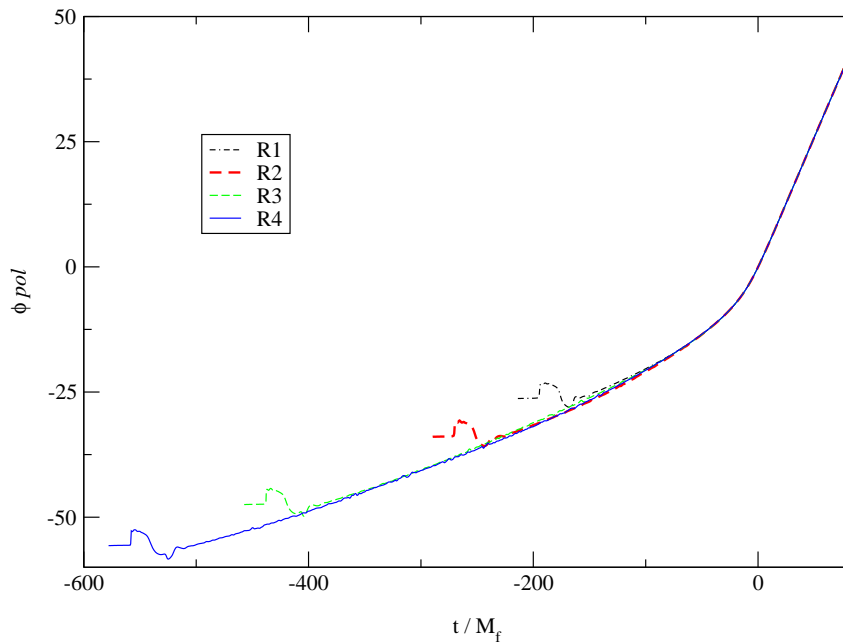
- $r\Psi_4(t)$ :  $L = 2, M = 2$  (the dominant mode).
- Excellent agreement among the runs for  $t > -50M_f$  at  $\sim 1\%$  level and errors are within 10% level prior to that.



# Results: Pol. Angle & Wave Freq.

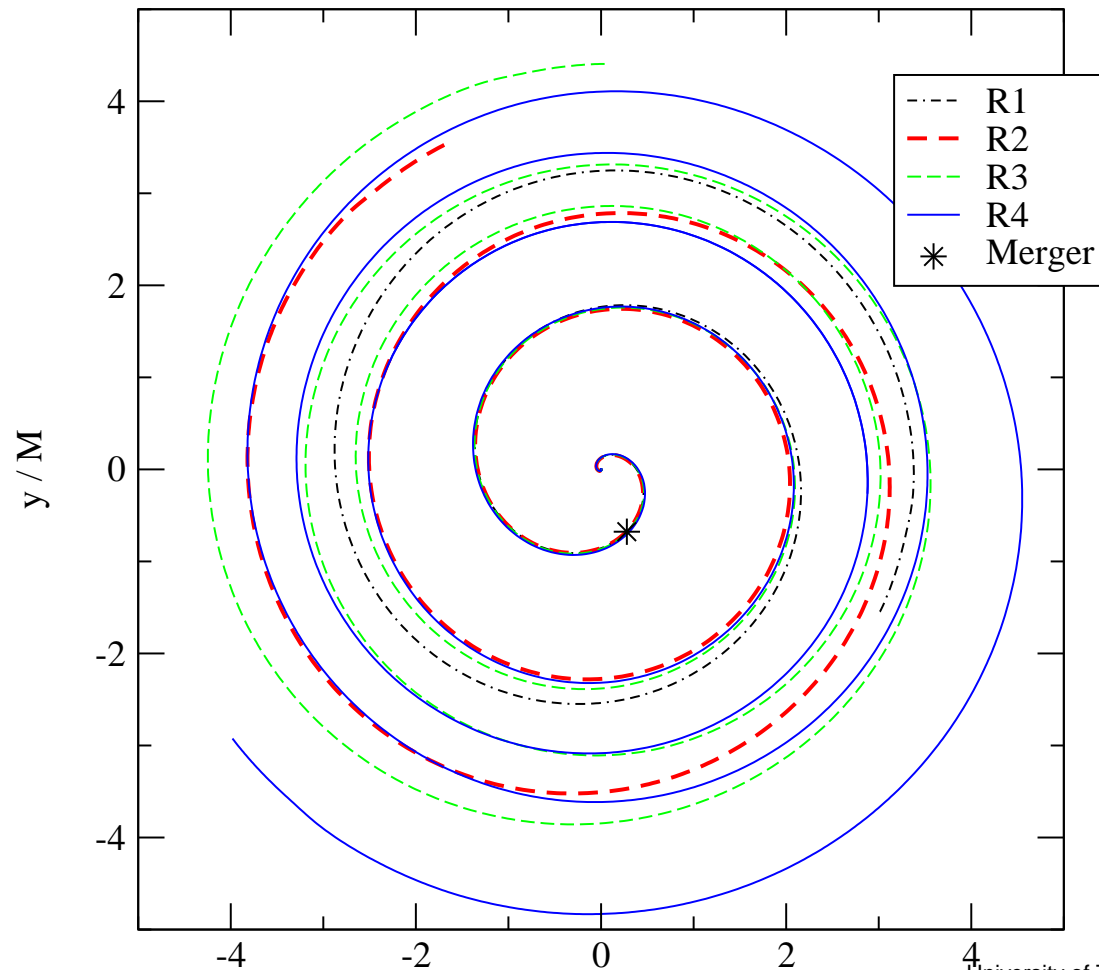
● Polarization angle,  $\varphi(t)$  ( $r\Psi_4(t) = A(t)\exp(-i\varphi(t))$ )

● Wave frequency  $\omega = \partial\varphi(t)/\partial t$  ( $M_{sun} \sim 5\mu s$ )



# Results: Puncture tracks from R1–R4

● “Puncture” trajectories:  $\dot{\vec{x}}_{punc} = -\vec{\beta}(\vec{x}_{punc})$



# Results: $E, J$ from R1–R4

- Energy and angular momenta for the radiation and final black hole.  $E_{rad}$  and  $J_{rad}$  are measured at  $r_{ex} = 30M$ , and  $r_{ex} = 50M$ , respectively.  $M_{QN}$  and  $a_{QN}$  are calculated independently from the quasi-normal fits of the ringdown waveforms, and agree well with the values deduced from the radiative losses.

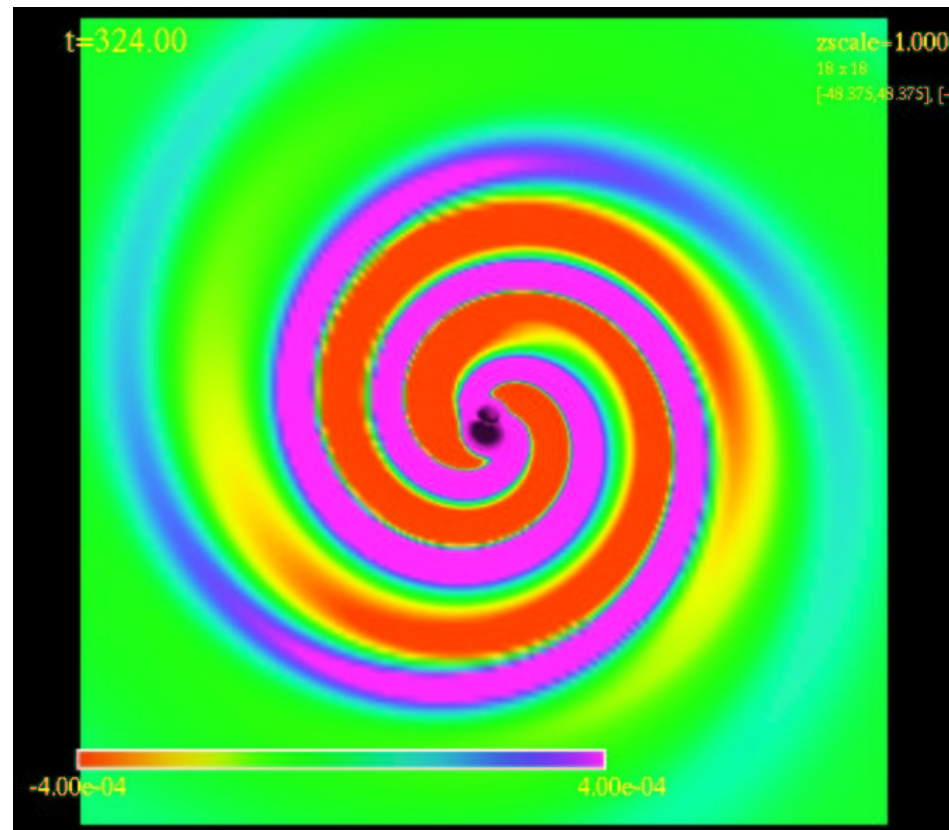
	$E_{rad}/M_f$	$J_{rad}/M_f^2$	$a/M_f$	$M_{QN}/M_f$	$a_{QN}/M_f$
<i>R1</i>	0.0356	0.246	0.694	1.005	0.721
<i>R2</i>	0.0369	0.272	0.691	1.002	0.686
<i>R3</i>	0.0381	0.306	0.689	1.004	0.694
<i>R4</i>	0.0387	0.325	0.702	1.004	0.693

# Results: Non-equal mass collision

- Motivation: asymmetric emission of GWs can impart astrophysical kick to the merger remnant.
- Large kick velocity can unbound the merged black hole from the center of the host structure → astrophysically very interesting value.
- Recent numerical calculations by Campanelli (2005) & PSU group (2006).
- Start with a simple case: mass ratio  $\rho = M_1/M_2 = 2/3 (= 0.667)$ .
- Mode analysis indicate that dominant contribution comes from  $L = 2, M = 2$  and  $L = 3, M = 3$  mixing.

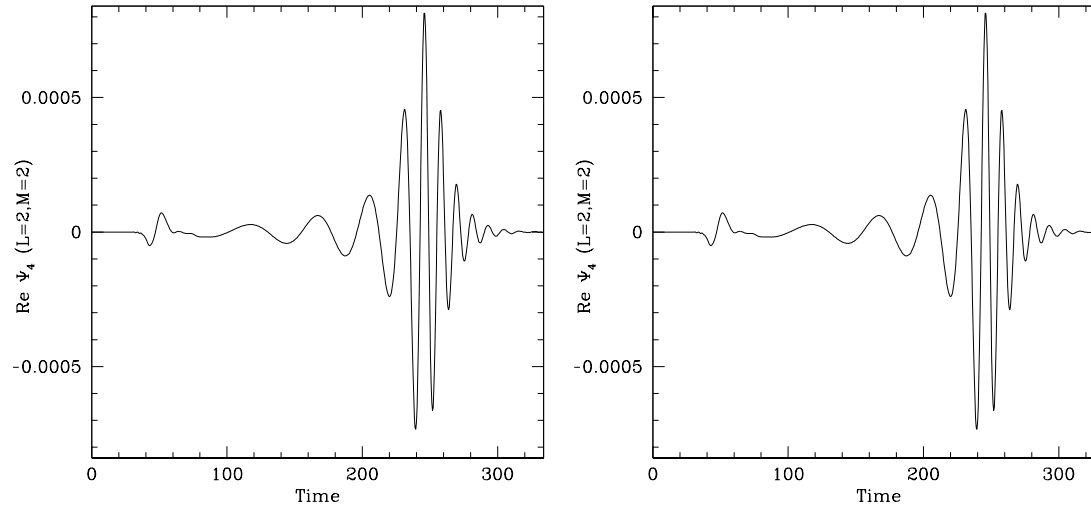
# Results: Non-equal mass collision, $\Psi_4$

- Initial separation  $\sim 9M$ ,  $h_f = M/21.3$
- $\Psi_4(t, x, y, z = 0)$  (real part) on  $Z = 0$  plane [MOVIE 3]
- $\Psi_4$  still dominated by  $L = 2, M = 2$  mode and asymmetry is a very subtle effect.



# Results: Non-equal mass collision: Kicks

- Waveforms at  $r_{ext} = 30M$ :  $L = 2, M = 2$  part and  $L = 3, M = 3$  part.



- $\omega_{22}/\omega_{33} \sim 2/3$ .
- Simulations with three different initial separation (coord separation of  $4.1M, 6.2M, 7.1M$ ) are used to analyze the final kick. ( $h_f = M/32, M/40, M/48$ )

- “kick” =  $v(t) = \frac{1}{M} \sqrt{\left(\int^t \frac{dP_x(t')}{dt'} dt'\right)^2 + \left(\int^t \frac{dP_y(t')}{dt'} dt'\right)^2}$

- Kick velocity  $\sim 105 \text{ km/s} \pm 10\%$  from the last orbit for  $\rho = M_1/M_2 = 2/3$ .

# Concluding Remarks

- Our results indicate gravitational waveform and trajectory analysis provide a consistent picture.
- Results shown in equal mass non-spinning binaries indicate that gravitational waveforms have universal features for the last orbit, merger, and ring-down.
- Early simulations to calculate gravitational radiation recoil kick are underway.
- Multiple groups working on BBH simulations (NASA/Goddard, UTB, Pretorius, PSU, LSU/AEI, Caltech/Cornell, FAU/UoJena etc).
- Future: large parameter space still to be explored (e.g. different mass ratio, spin, etc).